

Visualization of time-of-flight signals with normalized and calibrated phasor plot

Ryota Miyagi¹, Keiichiro Kagawa², Yuta Murakami¹, Hajime Nagahara³, Keita Yasutomi², and Shoji Kawahito²

¹ Graduate School of Integrated Science and Technology, Shizuoka University
3-5-1 Johoku, Nakaku, Hamamatsu, 432-8011 Japan

² Research Institute of Electronics, Shizuoka University
3-5-1 Johoku, Nakaku, Hamamatsu, 432-8011 Japan

³ Institute for Dataability Science, Osaka University
2-8 Yamadaoka, Suita, 565-0871 Japan

E-mail: rmiya@idl.rie.shizuoka.ac.jp

Abstract Impulse response signals with multi-path interference are measured by a highly-time-resolving CMOS image sensor for time-of-flight range imaging. They are analyzed and understood with a phasor plot method where frequency components are normalized by the total intensity and calibrated by a reference plane that describes a system function. In measurement, a silver-coated diffuser without sub-surface scattering is utilized as a reference. The phasor plots for different materials and open/closed environment are compared.

Keywords: Time-resolving CMOS image sensor, lateral electric field charge modulator, phasor plot, multi-path

1. Introduction

Lateral electric field charge modulator (LEFM)[1-3] has opened the pico-second regime ultra-high-speed computational imaging in a range of a few nano seconds or shorter, whose charge handling speed is close to the limitation of charge transfer speed in silicon. In this paper, we apply our time-resolving CMOS image sensor to measure the impulse response in environments and materials with multi-path interference. To visualize the multi-path interference, a normalized and calibrated phasor plot is used. Trajectories for multiple harmonics of time-domain complex frequency components for several materials are shown on the phasor plot to characterize the sub-surface scattering. Multiple reflections are visualized by the phasor plot for open and closed environments.

2. Normalized and calibrated phasor plot

Figure 1 depicts a typical environment with multi-path interference. The impulse response for such an environment is denoted by

$$f(\mathbf{r}; t) = \underbrace{\delta(t - \tau(\mathbf{r}))}_{\text{Direct}} * [\underbrace{\alpha + \beta h_{ss}(\mathbf{r}; t)}_{\text{Sub-surface scattering}}] + \underbrace{\gamma h_{mr}(\mathbf{r}; t)}_{\text{Multiple reflections}} \quad (1)$$

Phasor plot is used to visualize the impulse response on a two-dimensional complex plane[4-6]. Here, to remove intensity dependency and a system function (temporal waveform of excitation light, sensor response, and systematic delay caused by the electric and optical path length).

Assumed that an optical signal and a system function are given by $f(t)$ and $h(t)$, respectively, the measured signal, $g(t)$, is written as

$$g(t) = f(t) * h(t) \quad (2)$$

In this paper, the frequency component is normalized and calibrated as follows

$$F_{NC}(\nu) = \left[\frac{G(\nu) / \sum g(t)}{H(\nu) / \sum h(t)} \right]^* \quad (3)$$

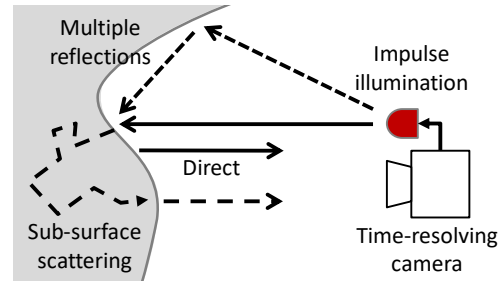


Fig. 1. Multi-path interference in time-of-flight depth imaging.

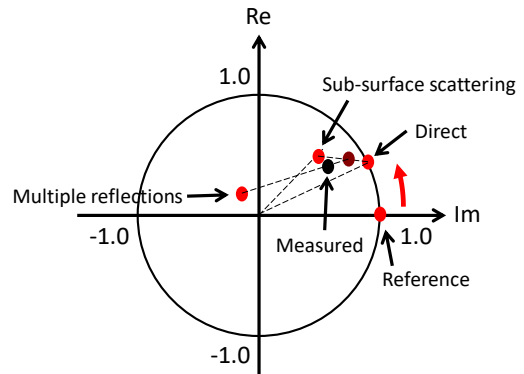


Fig. 2. Multi-path interference in normalized and calibrated phasor plot.

Note that x^* means the complex conjugate of a complex value, x . Figure 2 illustrates how multi-path interference is shown in the phasor plot. Direct signal is on the circle with a radius of unity. If an object is placed further from the camera, the angle rotates anticlockwise. Sub-surface scattering rotates the measure point anticlockwise and reduces the amplitude. Because multiple reflections tend to have a long path length and the pulse is widened significantly, a measured point can have a large rotation angle and a small amplitude. The measured point becomes a linear combination of signal components. The point, $1.0+0i$, corresponds to the reference plane.

3. Experimental results

In experiments, a time-resolving CMOS image sensor designed for fluorescence lifetime imaging was utilized[2]. To

achieve the time-resolved imaging, images were captured with the time window gradually shifted. As an impulse light source, super continuum laser (NKT, SuperK Extreme EXB-6, 19.49MHz with a pulse picker) was used and a wavelength of 650nm by a bandpass filter of 650nm \times 25nm was inserted. 33 images were captured with a unit delay of 159.375ps and inter-frame subtraction was performed to reproduce transient images. Thus, the measured time range was 5.1ns. As a reference, a silver-coated diffuser was used because it has no sub-surface scattering.

The trajectories for several materials are shown in Fig. 4. Cork and the white plastic plate showed the smallest and largest rotation angles, respectively. It can be because cork has a large absorption and the optical path length is small. On the other hand, the white plastic plate is diffusive and absorption is very weak, so that the optical path length becomes very long.

A dice was measured in an open space, in which there is no multiple reflections, and a closed space where the dice was surrounded by six white plastic plates whose size was 100m \times 100mm \times 2mm (thickness). Figure 5 shows a situation of the closed environment. Excitation light was introduced through the hole of the front plate. Figure 5 compares the phasor plots for the open and closed environments. In the open space, only one peak caused by the dice was observed in the phasor plot slightly inside the unity circle due to sub-surface scattering. However, in the closed environment, multiple distributions are observed due to multiple reflections. Note that “dice for open” is superimposed for comparison.

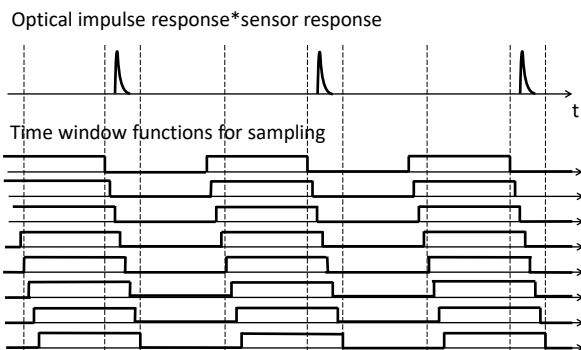


Fig. 3. Sliding time windows for time-resolved imaging.

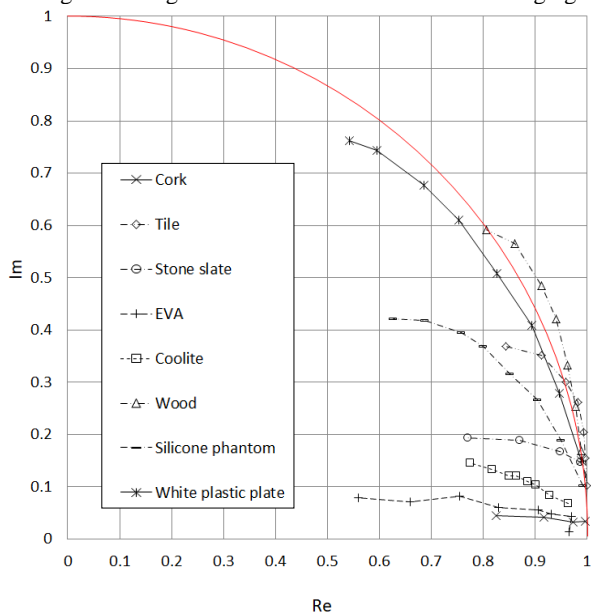


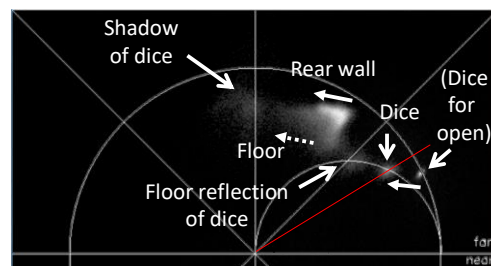
Fig. 4. Trajectories for several materials. The harmonics orders from 1 to 8 are shown.



Fig. 5. A dice in a closed space.



(a) Open



(b) Closed

Fig. 6. Phasor plots for the 1st order harmonics of a dice placed in open and closed environments.

4. Conclusion

Normalized and calibrated phasor plot was described in this paper. Multi-path interference was visualized by the modified phasor plot in two cases: sub-surface scattering of several materials and a dice in open/closed environment.

Acknowledgements

This work was partially supported by Grant-in-Aid for Scientific Research (S) Numbers 17H016012 and 18H05240, and Regional Innovation Ecosystem Program.

References

- [1] S. Kawahito, G. Baek, Z. Li, S. Han, M. Seo, K. Yasutomi and K. Kagawa, “CMOS lock-in pixel image sensors with lateral electric field control for time-resolved imaging,” *International Image Sensor Workshop*, 10.06, pp. 1417-1429 (2013).
- [2] M. -W. Seo, K. Kagawa, K. Yasutomi, T. Takasawa, Y. Kawata, N. Teranishi, Z. Li, I. A. Halin, S. Kawahito, “A 10.8ps-time-resolution 256x512 image sensor with 2-tap true-CDS lock-in pixels for fluorescence lifetime imaging,” *ISSCC Dig. Tech. Papers*, pp. 189-199 (2015).
- [3] M. -W. Seo, Y. Shirakawa, Y. Masuda, Y. Kawata, K. Kagawa, K. Yasutomi, S. Kawahito, “A programmable sub-nanosecond time-gated 4-tap lock-in pixel CMOS image sensor for real-time fluorescence lifetime imaging microscopy,” *ISSCC Dig. Tech. Papers*, pp. 70-71 (2017).
- [4] R. Colyer, C. Lee and E. Gratton, “A novel fluorescence lifetime imaging system that optimizes photon efficiency,” *Microscopy Res. and Tech.* **71**, pp. 201-213 (2008).
- [5] D. Suzuki, K. Tanaka, K. Kitano, T. Funatomi, and Y. Mukaigawa, *IPJS SIG Tech. Rep.*, Vol. 2018-CVIM-210, No. 49, pp. 1-8 (2018, in Japanese).
- [6] M. Gupta, S. Nayar, M. Hullin, and J. Martin, “Phasor imaging: a generalization of correlation-based time-of-flight imaging,” *ACM Trans. Graphics* **34**, Article 156 (2015).